Thermal Design, Analysis, and Sensitivity of a Sample Tube on the Martian Surface

Matthew Redmond[1], Sarah Sherman[2], Pradeep Bhandari[3], and Keith Novak[4]
NASA Jet Propulsion Laboratory, California Institute of Technology, Pasadena, CA, 91109, USA

NASA will launch a rover to Mars in 2020 to collect and cache samples of Martian rocks and regolith for potential return to Earth on a future mission. The collected samples will be placed in tubes, hermetically sealed, and deposited on the surface of Mars for a period of up to 10 years. Preventing the deposited samples from overheating is an important consideration in order to ensure their scientific integrity. The samples are required to remain below 60 °C, however there is a goal to keep them below 40 °C. This temperature requirement is challenging, considering that the maximum surface temperature of Mars is 38 °C and the tube must be thermally controlled through only passive means. As a result, a significant effort has been made to design a tube to contain the samples and investigate innovative tube surface treatments that maintain proper sample temperatures without significant adverse effects of sample contamination. The tube uses a specialized aluminum oxide coating to prevent overheating on the Martian surface. The maximum predicted tube temperature is relatively insensitive to local thermal inertia, ground contact, and ground slope, but is very sensitive to landing site latitude and dust deposition. The maximum predicted sample temperature in the +/- 30° landing latitude range with worst case assumptions is 54 °C, but many of the potential landing sites have significantly cooler maximum predicted sample temperatures. This paper describes the thermal design, analysis, and sensitivity studies performed on the sample tubes and also discusses operational considerations.

Nomenclature

A	= albedo	*ACA*	= Adaptive Caching Assembly
D	= diameter	*CCMD*	= Caching Component Mounting Deck
G	= conductance	*DDR*	= Detailed Design Review
L	= length	*Ls*	= Solar Longitude
h	= convection coefficient	*MSL*	= Mars Science Laboratory
T	= tube temperature	*RA*	= Robotic Arm
T_G	= ground temperature	*RTG*	= Radioisotope Thermoelectric Generator
T_A	= atmospheric temperature	*SCS*	= Sample Caching System
T_S	= sky temperature	*SHA*	= Sample Handling Arm
Q	= heat flow	*Tau*	= Atmospheric Optical Depth
$q''_{diffuse}$	= diffuse component of the solar flux	*TES*	= Thermal Emission Spectrometer
q''_{direct}	= direct component of the solar flux	*TI*	= Thermal Inertia
α	= solar absorptivity	*WCH*	= Worst Case Hot
ε	= thermal emissivity		
π	= pi		
σ	= stefan boltzman constant		
ϕ	= ground slope angle		
θ	= solar elevation angle		

[1] Thermal Engineer, Instrument and Payload Thermal Engineering.
[2] Mechatronics Engineer, Mechanical Systems and Technology.
[3] Principal Engineer, Propulsion, Thermal, and Materials Systems.
[4] Principal Engineer, Spacecraft Thermal Engineering.

Introduction

THE Mars 2020 rover is currently proposed to launch in 2020 and land on Mars at a latitude of between 30° N and 30° S in the year 2021. This new rover is based on the Mars Science Laboratory (MSL) rover, Curiosity, which successfully landed on Mars in 2012 and is currently exploring the surface. The new rover will carry more sophisticated science instruments in order to determine the potential habitability of Mars and look for signs of ancient Martian life. The selected rover instruments are listed below[1], and shown in Figure 1.

- *Mastcam-Z*: An advanced zoom-capable camera with the ability to study the mineralogy of Mars and assist with rover operations.
- *SuperCam:* An instrument capable of imaging, chemical composition analysis, minerology, and remote detection of organic compounds.
- *PIXL*: An X-ray fluorescence spectrometer that would map fine scale elemental composition.
- *SHERLOC*: A spectrometer used to map fine-scale mineralogy and detect organic compounds.
- *MOXIE*: An exploration technology demonstration that would convert Martian Carbon Dioxide into Oxygen.
- *MEDA*: A set of sensors that measure temperature, wind speed, pressure, humidity, and atmospheric dust.
- *RIMFAX*: Ground penetrating radar that would provide centimeter-scale resolution of the geologic structure of the subsurface.

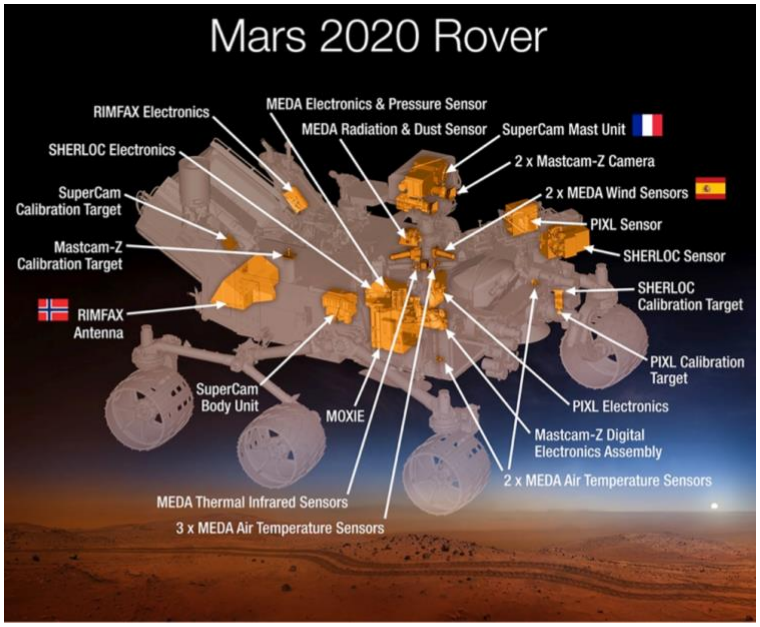

Figure 1. Selected instruments for the Mars 2020 Rover[1].

These instruments are designed to complement and inform another major component of the Mars 2020 Rover: a sample caching system (SCS), which includes an Adaptive Caching Assembly (ACA). The SCS and ACA are shown in Figure 2, and will collect, seal, and cache samples of Martian rocks and regolith for potential return to Earth on a future mission. The collected sample size is approximately 10 cc in volume and 15 grams in mass. The exact sequence of events is still in work, but in general sample collection begins when a sample tube is removed from sample tube storage by the sample handling arm (SHA). An end effector on the end of the SHA is used to grip and release the sample tube. The SHA then inserts the sample tube into a drill bit stored inside the bit carousel. The bit carousel transports the bit and exchanges it with the robotic arm (RA). The RA has a turret on the end with a drill, which receives the sample tube and bit during bit exchange. The RA places the drill on a scientifically interesting location, and a regolith or rock sample is collected. The sample tube and bit, which now contains a collected sample, is exchanged again using the bit carousel and the sample tube is retrieved by the SHA. At this point, the rest of the operations take place inside the adaptive caching assembly (ACA). The SHA transports the sample tube to the volume and vision stations, where sample volume is measured and images are taken. Hermetic seals are dispensed into the tube, and a sealing station is used to hermetically seal the sample inside of the sample tube. Once the sample is collected and sealed, it is stored in tube storage where it will remain until a decision is made to cache the collected samples by the rover science team. To cache a sample tube, the SHA will use the tube drop off station to drop the tube onto the ground through a large belly pan opening underneath the entire ACA.

The current plan is for samples to be cached in a depot for possible future collection and return to Earth. This process of sample collection and caching has been termed "depot caching" and is illustrated graphically in Figure 3. The rover will land and travel to one or more regions of scientific interest to collect samples. It will then cache the collected samples on the ground before traveling to other regions of interest to collect additional samples as part of a possible extended mission. Once a sample is collected, it could remain on the surface of Mars for up to 10 years. Some of the proposed methods which might be used to return a Mars sample to Earth involve placing the sample in orbit around Mars and in transit back to Earth for up to an additional 10 years.

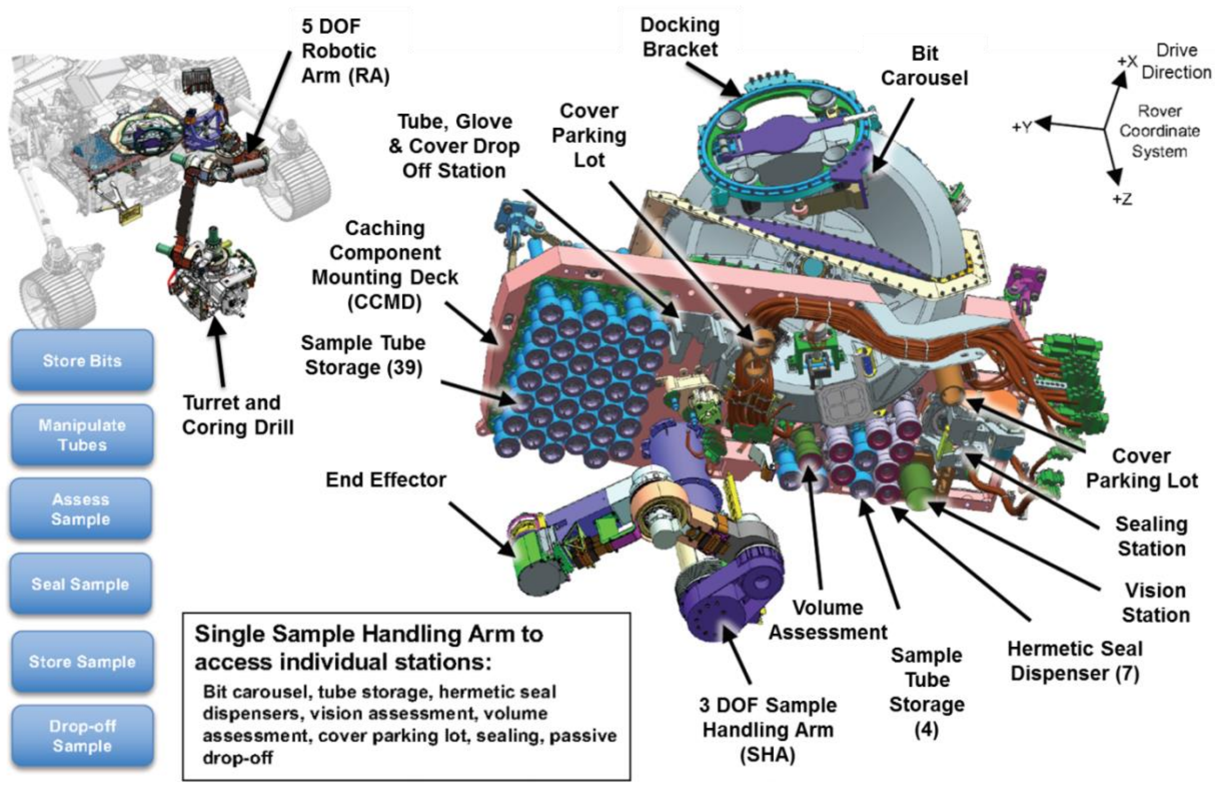

Figure 2. Sample Caching System (SCS) and Adaptive Caching Assembly (ACA) on the Mars 2020 Rover.

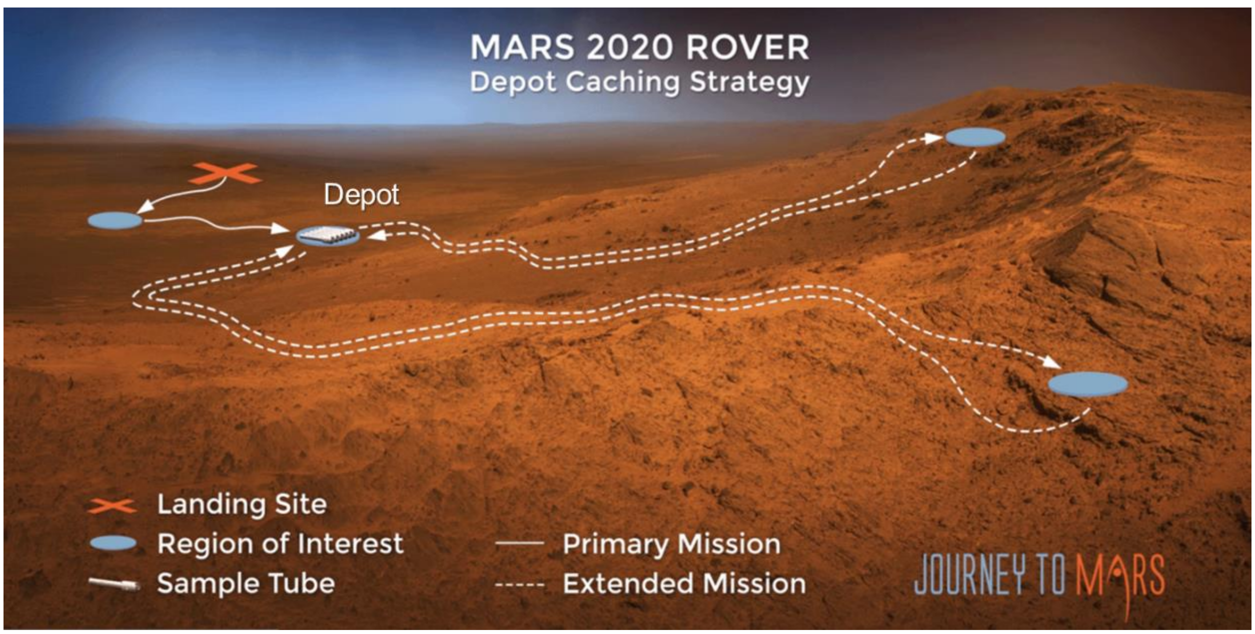

Figure 3. Graphical illustration of the Mars 2020 rover depot caching strategy[2].

Because of the substantial scientific value of collected samples, great care needs to be taken to ensure the samples maintain their scientific integrity[3,4]. For example, the samples will be stored in individual, hermetically sealed sample tubes to minimize cross contamination between samples and prevent the escape of water vapor[5]. The tubes also serve to maintain sample integrity and prevent disaggregation during the violent launch and landing events which would be experienced on the way back to Earth[6,7]. In addition, stringent limits on biologic, organic, and inorganic contaminants have been placed on any hardware that interacts with the samples, which includes the tubes[3,4]. Finally, preventing the deposited samples from overheating is an important consideration in order to ensure their scientific integrity. This topic of sample heating has been briefly discussed in a preliminary way in previous papers[5-7], but is dealt with in greater depth in this paper.

I. Sample Temperature Requirements

Sample temperature requirements were formulated by the Returned Sample Science Board (RSSB) in consideration of 11 scientific investigations where elevated temperatures could have a detrimental effect on the science results[8]. A chart summarizing the acceptable temperature range for the 11 science investigations is shown in Figure 4. From the chart, it is clear that maximum sample temperatures in the range of 40 to 60 °C are acceptable to the investigations considered. The Mars 2020 project has been instructed to ensure that every part of collected samples remain below 60 °C. The engineering team is also taking efforts to keep the samples as cool as possible, with a goal of keeping every part of the collected samples below 40 °C. This temperature requirement and goal is challenging considering that the maximum surface temperature of Mars is 38 °C and the tube must be thermally controlled through only passive means. There is no minimum sample temperature requirement, although the sample tube and hermetic seal assembly is being qualified down to a minimum temperature of -135 °C.

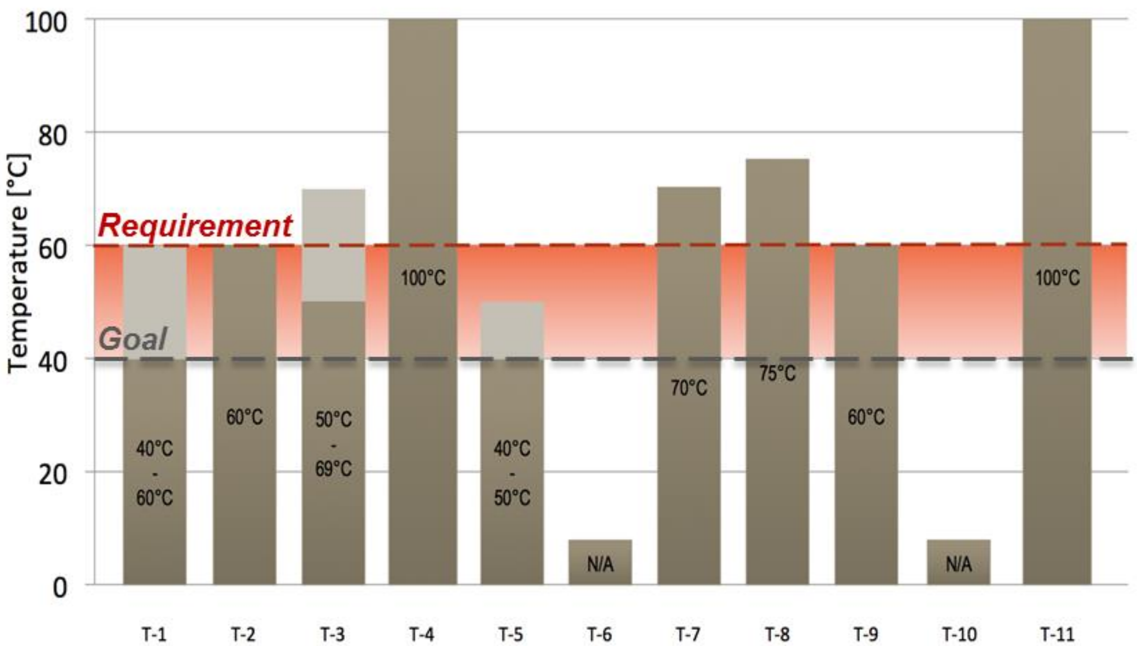

Figure 4: Maximum allowed temperature ranges for 11 temperature sensitive scientific investigations[8].

II. Thermal Environments

A total of five thermal environments were used for this work. One worst case hot (WCH) detailed environment was used, and four approximate summertime environments were used. The WCH detailed environment was obtained from a Mars Climate Model, and the approximate environments were obtained through a combination of climate models and interpolation/extrapolation of their results, which is why we stress their approximate nature. The WCH environment is shown in Figure 5. The WCH 27°S environment is a worst case combination of latitude, atmospheric optical depth, albedo, and ground thermal inertia that produces warmer ground and atmospheric temperatures than any potential landing site on the surface of Mars, and has been used in prior projects at JPL[5,9-11]. The actual landing site selected is unlikely to be as extreme as this one, but this environment is used for tube thermal analysis because the Mars 2020 rover is required to be able to land and perform its mission at any landing site within the +/- 30° latitude range. A topographic map depicting the top 8 landing sites[12] under consideration for Mars 2020 is shown in Figure 6. Furthermore, the top 3 landing sites were selected from these 8 at a recent landing site workshop[13].

The four approximate environments were used to approximate the summertime tube temperatures at the latitudes of 15°S, 0°, 15°N, and 30°N and get an idea of how sensitive peak tube temperature is to landing site selection. Due to the orbital eccentricity and obliquity of Mars, peak ground temperatures occur near Ls 270 in the southern hemisphere and equatorial regions and near Ls 90 in the northern hemisphere regions. Using these approximate environments reduced the amount of analysis necessary compared to what would be required if an analysis was performed for every possible landing site. This approximation is acceptable due to the bounding nature of the WCH 27°S environment. Approximate peak diurnal boundary conditions for all five environments are summarized in Table 1, and a contour plot of the maximum annual observed surface temperatures on the surface of Mars, as measured by the Thermal Emission Spectrometer (TES) instrument on Mars Global Surveyor, is shown in Figure 7. The table and maximum annual observed surface temperatures correspond well to one another.

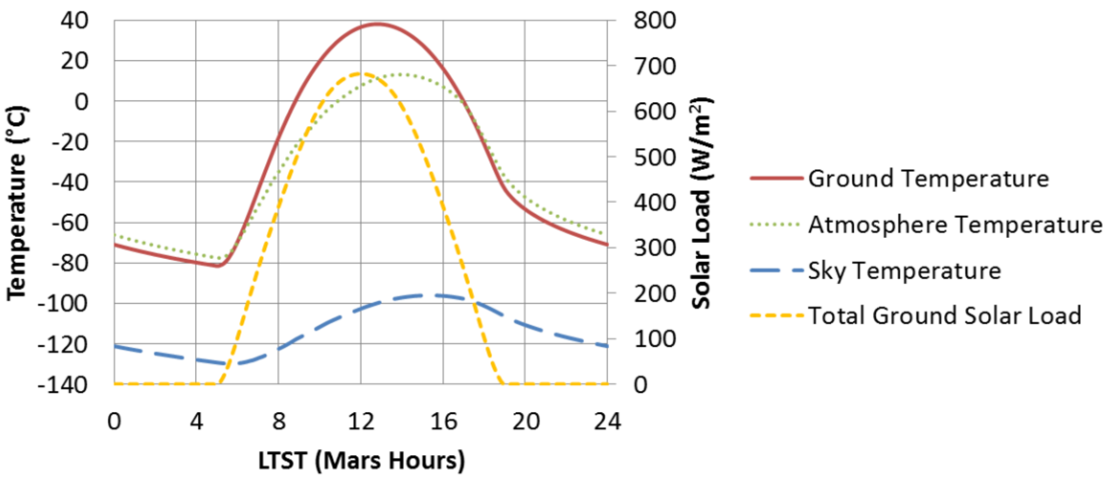

Figure 5: The worst case hot (WCH) environment used in the analysis. The latitude is 27°S, with atmospheric optical depth of 0.2, albedo of 0.12, and thermal inertia of 220 Jm-2K-1s-1/2.

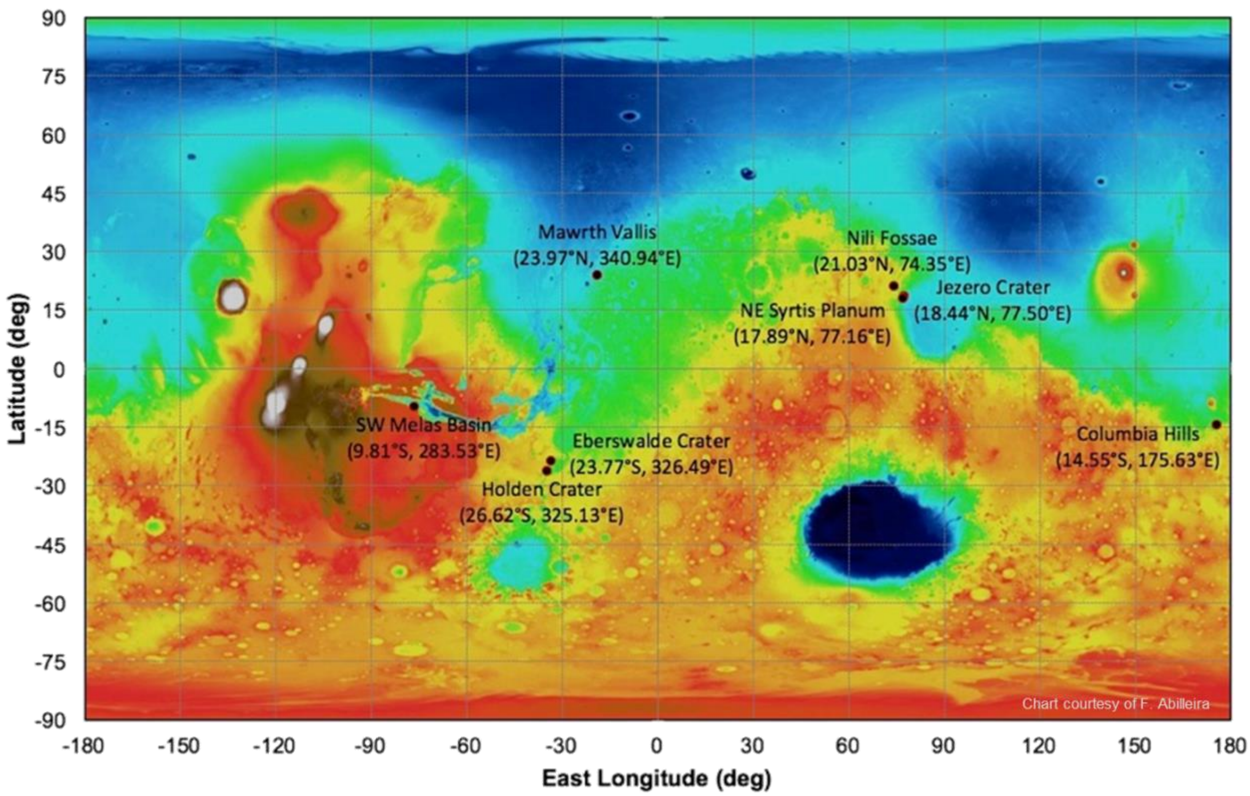

Figure 6: Topographic map depicting the top 8 landing sites under consideration for Mars 2020.

Table 1: Approximate peak diurnal boundary conditions for all five environments used in this paper.

Latitude	Ls (degrees)	T_G (°C)	T_A (°C)	T_S (°C)	$q''_{diffuse}$ (W/m^2)	q''_{direct} (W/m^2)	Θ (degrees)
WCH 27 °S	270	38	13	-96	103	582	88
15 °S	270	28	2	-104	103	572	80
0 °	270	17	7	-105	103	517	65
15 °N	90	1	-8	-105	72	402	80
30 °N	90	3	-8	-105	72	408	85

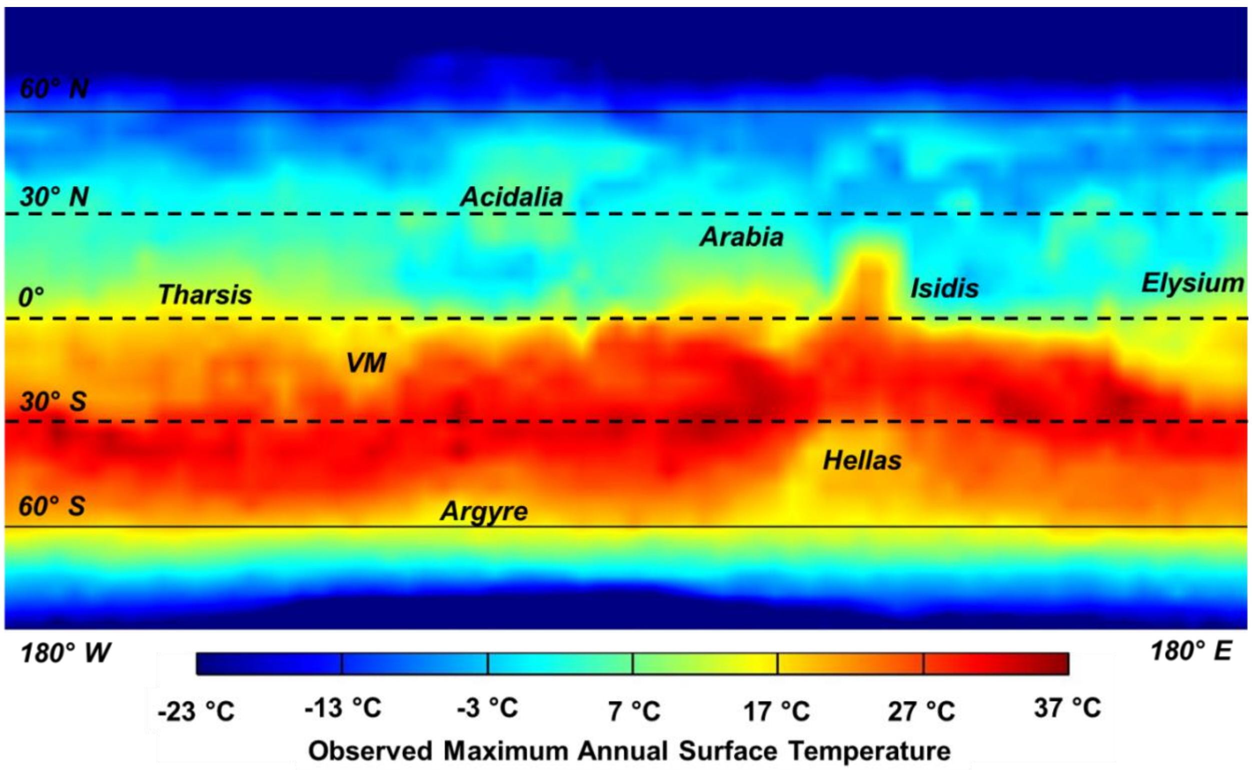

Figure 7: Maximum annual observed surface temperatures on the surface of Mars as measured by the TES instrument.

III. Tube Surface Treatments and Optical Property Measurements

A number of sample tube surface treatments were considered, and optical property measurements were taken for many of these surface treatments. Table 2 summarizes the optical property measurements and literature values which were used in this work. Multiple vendors were asked to make coupons for testing, so that a final process could be selected. Solar absorptivity and thermal emissivity measurements were taken using a TESA 2000 reflectometer.

In the initial tube design, a bare metallic external tube surface was desired for its simplicity, ease of handling, and ability to meet the stringent cleanliness requirements for sample collection. However, thermal analysis indicated that a bare metallic or even a grit blasted metallic surface may not have a sufficiently high emissivity to keep the sample below the 60 °C temperature requirement. As a result, alternative surface treatments were explored, including oxidizing and anodizing. These surface treatments, like grit blasting, also were not able to guarantee that the temperature requirements would be met. Titanium nitriding also was explored, not as a thermal control coating, but as a way to improve the cleanliness and decrease contamination on the tubes. From a thermal engineering standpoint, the ideal coating would be white paint, however concerns regarding paint particle shedding and contamination of the collected samples eliminated white paint from consideration. Instead, using high purity flame sprayed Aluminum Oxide (Al_2O_3) coating was explored. Aluminum Oxide is a very hard, very tough ceramic with a white appearance. It is very good for thermal control due to its high emissivity and relatively low solar absorptivity. In addition, high purity Aluminum Oxide would pose minimal contamination risk to collected Martian samples. If particle shedding were to contaminate the samples, it could be identified as a contaminant, as opposed to a native mineral during scientific examination of any possible returned Martian sample tubes. Surface treatments and coatings planned for use on the flight design are shown in green bold text in Table 2 below.

Table 2: Summary of optical properties considered (black text) or planned (green text) for use on the flight design. All values are measured values except for those which reference a source in the literature.

Surface Treatment or Coating	Solar Absorptivity	Thermal Emissivity
3 mil Flame Sprayed Aluminum Oxide (Al_2O_3), ABS	0.41 to 0.49	0.83 to 0.85
3 mil Flame Sprayed Aluminum Oxide (Al_2O_3), Surface Modification Systems	0.23 to 0.35	0.81 to 0.82
Polished Flame Sprayed Aluminum Oxide (Al_2O_3)	0.39 to 0.69	0.76 to 0.85
Grit Blasted Stainless Steel, Surface Optics Corp	0.58[14]	0.38[14] to 0.49
Grit Blasted Aluminum, Peen Rite	0.24 to 0.48	0.13 to 0.29
Grit Blasted Titanium, Surface Optics Corp	0.80[15] to 0.88[15]	0.46[15] to 0.60
Bare Titanium	0.48 to 0.66	0.16 to 0.20
Oxidized Titanium, After 500 C Bake Out	0.70 to 0.77	0.20 to 0.22
Titanium Nitride (TiN), Brycoat	0.36 to 0.38	0.07 to 0.11
Titanium Nitride (TiN), Solar Atmospheres	0.45 to 0.52	0.16 to 0.18
Titanium Anodize, Tiodize, Type II	0.82 to 0.84	0.45 to 0.51
Titanium Anodize, Danco, Type II	0.80 to 0.83	0.36 to 0.41
Titanium Anodize, Tiodize K2V	0.91	0.86
Titanium Anodize, Tiodize Type IV (Type II + X40 PTFE “Teflon Infused”)	0.85	0.45

IV. Closed Form Model

During the design process, a closed form thermal model was used to quickly estimate sample tube temperatures in the WCH 27°S environment. This closed form model was also used to validate more complex computer models which were used at later stages in the design process. The tube can be approximated as an infinite cylinder, and an energy balance can be performed using all the boundary conditions, as summarized in Figure 8 and Equations 1 to 4. This closed form model makes the following assumptions, all of which are hot biased and therefore conservative:

- Free convection only (~ 0.4 W/m^2-K, hot biased)
- Worst case dust coverage with 100% dust (hot biased)
- Tube is placed on flat ground (hot biased at WCH 27°S environment)
- Tube is not in contact with the ground (hot biased)

One of the key assumptions is the dust coverage assumption. Samples would be left on the surface of Mars for up to 10 years, which could increase the solar absorptivity of the tubes to as high as 0.7 due to dust collection since solar wavelengths (~ 0.5 µm) are comparable to the length scale of Martian dust particles (~ 1-2 µm)[16]. However, the thermal emissivity of the sample tubes may not be affected by dust since the IR wavelengths (~ 5 - 40 µm) are much larger than the length scale of Martian dust particles. The tube absorptivity and emissivity dictate maximum tube temperatures, but since the absorptivity can be increased due to dust deposition it is the tube emissivity that is of primary importance. In addition, it is interesting to note that this predicted temperature of the tube is independent of the tube dimensions, as indicated by the simplification which takes place from Equations 3 to 4.

$$Q_{in} = Q_{out} \tag{1}$$

$$Q_{DirectSolar} + Q_{DirectReflectedSolar} + Q_{DiffuseSolar} + Q_{DiffuseReflectedSolar} + Q_{GroundIR} + Q_{SkyIR} + Q_{Convection,In} = Q_{Convection,Out} + Q_{Emitted} \tag{2}$$

$$q''_{direct}\alpha DL + q''_{direct}\sin(\theta)\, A\alpha\frac{\pi DL}{2} + q''_{diffuse}\alpha\frac{\pi DL}{2} + q''_{diffuse}A\alpha\frac{\pi DL}{2} + \frac{\pi DL}{2}\sigma\epsilon T_G^4 + \frac{\pi DL}{2}\sigma\epsilon T_S^4 + h(\pi DL)T_A = h(\pi DL)T + (\pi DL)\,\sigma\epsilon T^4 \tag{3}$$

$$q''_{direct}\alpha + q''_{direct}\sin(\theta)\, A\alpha\frac{\pi}{2} + q''_{diffuse}\alpha\frac{\pi}{2} + q''_{diffuse}A\alpha\frac{\pi}{2} + \frac{\pi}{2}\sigma\epsilon T_G^4 + \frac{\pi}{2}\sigma\epsilon T_S^4 + h\pi T_A = h\pi T + \pi\sigma\epsilon T^4 \tag{4}$$

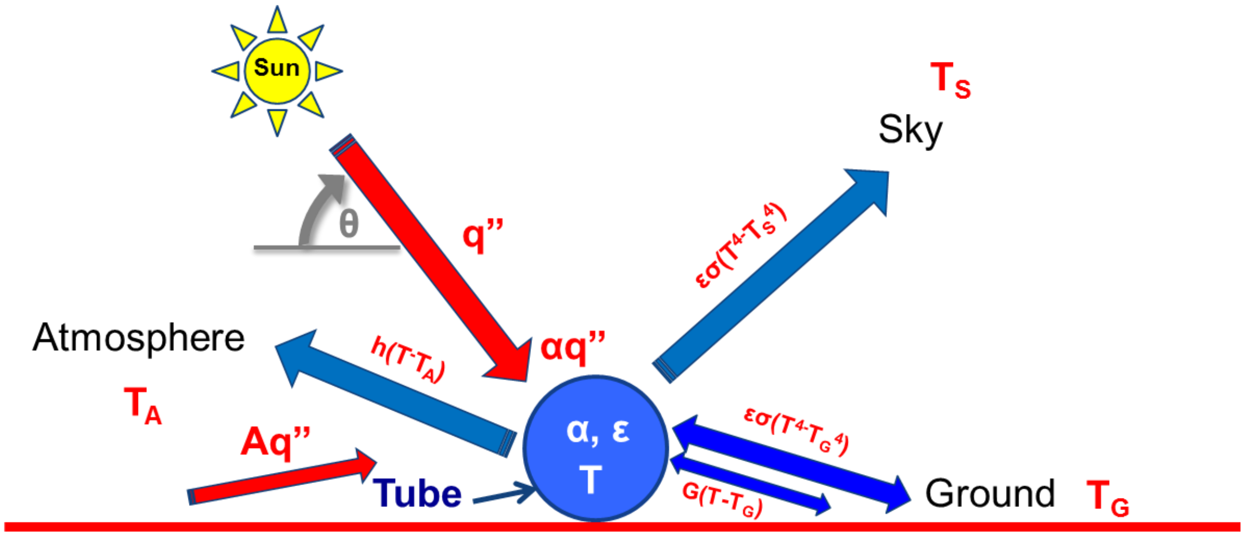

Figure 8: Sample tube boundary conditions for closed form model.

V. Detailed Models

Detailed computer models were also used to estimate the diurnal tube temperature using transient models of the Martian environment. The detailed computer models were able to account for variables which were not present in the simple model. In the detailed models, the ground underneath the sample tube was explicitly modeled, which allows the ground temperature to be influenced by shadowing effects, ground slope, ground thermal inertia, and albedo. The ground was modeled using a 1 m thick solid, with 0.5 mm thick discretization near the surface, 1 cm thick discretization in the upper 10 cm, and 2 cm thick discretization for depths greater than 10 cm. A 1.5 W/m^2-K convection coefficient is used between the ground surface and the atmospheric temperature. This same approach has been validated for use with the Mars 2020 rover thermal model[11].

A number of different detailed computer models were used for this work. As the tube design matured, additional details were added to these models. The detailed models used similar assumptions as the simplified model, but with a few exceptions. Assumptions are listed below:

- Free convection only (~ 0.4 W/m^2-K, hot biased)
- Worst case dust coverage with 100% dust (hot biased)
- Tube is assumed to be empty (produces maximum gradients and hot biased local temperatures)
- Tube is placed on ground with varying degrees of ground slope (0 to 30°)
- Tube is placed in varying degrees of contact with ground (hovering to perfect contact)
- Tube is placed on ground with varying albedo (*A* = 0.12 to 0.30)
- Tube is placed on ground with varying thermal inertia (TI= 220 to 350 $Jm^{-2}K^{-1}s^{-1/2}$)

The assumptions of free convection only and worst case dust coverage are identical to those made in the simplified model. In addition, the detailed models had the capability to model gradients in the tube. As a result, the tube was assumed to be empty. This results in the most extreme gradients as well as hot biased local temperatures. This assumption is conservative, but it was also made out of necessity since it is not possible to know the shape, rock type, and thermal contact resistance of the samples that will be collected on Mars. Predicted sample temperature are inferred from the model results by assuming that the sample could reach the same temperatures as any portion of the tube that the sample could be in contact with. The detailed models were used to perform a number of sensitivity studies, as well as the worst case hot temperature predictions of the flight tube design. By default, the tubes were assumed to be placed on flat ground, with no ground contact, free convection only, a ground albedo of 0.12 and a ground thermal inertia of 220 $Jm^{-2}K^{-1}s^{-1/2}$ unless noted otherwise. Screenshots of several detailed tube models are shown in Figure 9.

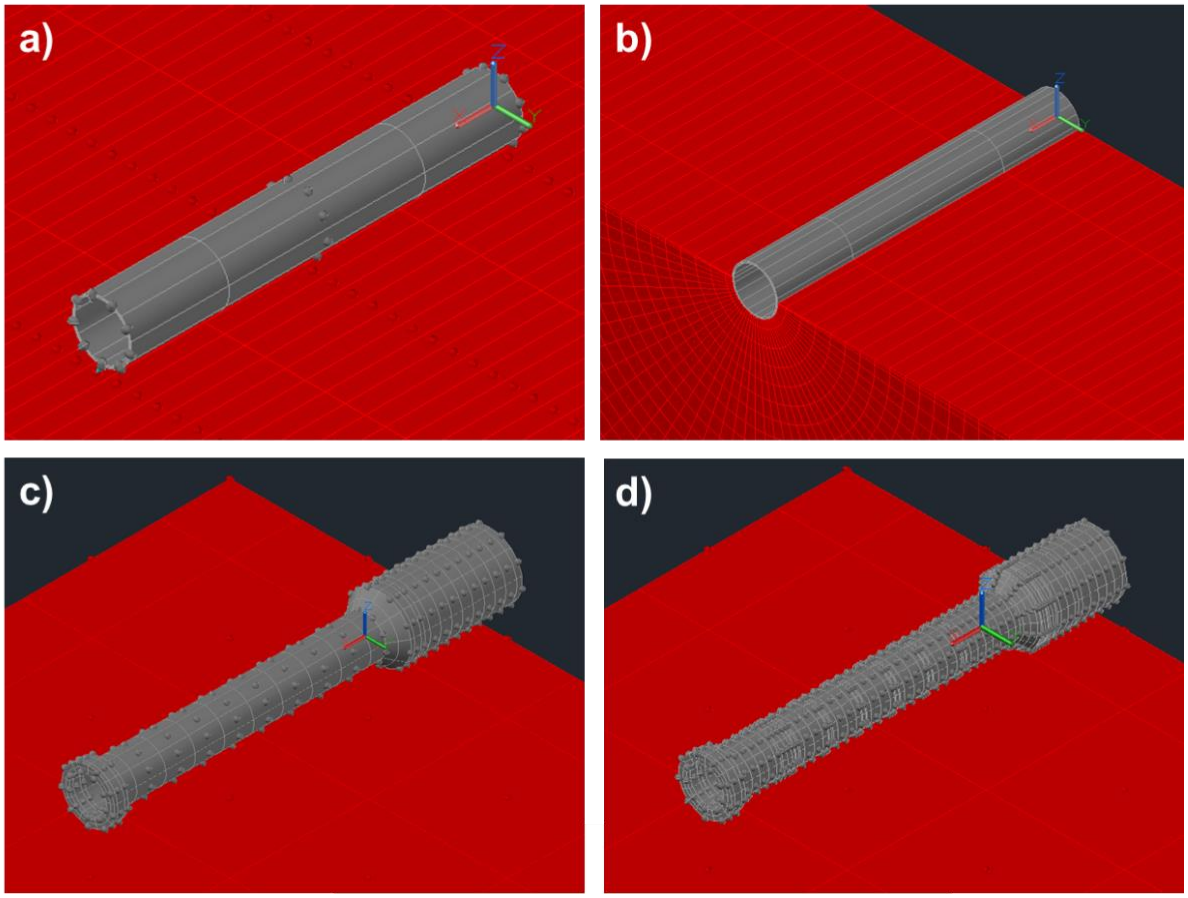

Figure 9: Screenshots of several detailed tube models used for tube and sample temperature predictions: a) simplified tube on ground model, b) simplified tube embedded in ground model, c) moderate level of detail tube on ground model, d) detailed tube on ground model.

VI. Sensitivity Studies

Sensitivity studies were given significant weight in the sample tube thermal design process. One of the first sensitivity studies that was performed was a sensitivity of tube temperature for different coatings in the WCH 27°S environment. Using the closed form model (Section IV), tube temperatures were predicted for 25 different combinations of thermal emissivity and solar absorptivity. The results could then be used to estimate the WCH 27°S tube temperature for any surface treatment under consideration. A chart showing the sensitivity study results with candidate surface treatments is shown in Figure 10. Peak tube temperature can be strongly affected by the solar absorptivity of the tube, which is strongly affected by dust deposition. However, it is not realistic to attempt to control the amount of dust deposited on the tube over its 10 year mission lifetime. Therefore a solar absorptivity of 0.7, corresponding to 100% dust coverage, is assumed for all potential surface treatments, except for those that have a BOL solar absorptivity of greater than 0.7. With a fixed solar absorptivity of dust (0.7), the thermal emissivity of the tube needs to be greater than ~0.45 to meet the 60 °C sample temperature requirement and greater than ~0.75 to meet the 40 °C sample temperature goal in the WCH 27°S environment. It is clear that TiN, bare titanium, and oxidized titanium would not even come close to meeting the temperature requirement. Anodized titanium, grit blasted titanium, and grit blasted stainless steel might meet the temperature requirement. Of all the surface treatments, only flame sprayed aluminum oxide would allow the sample to meet its sample temperature requirement and possibly meet its temperature goal.

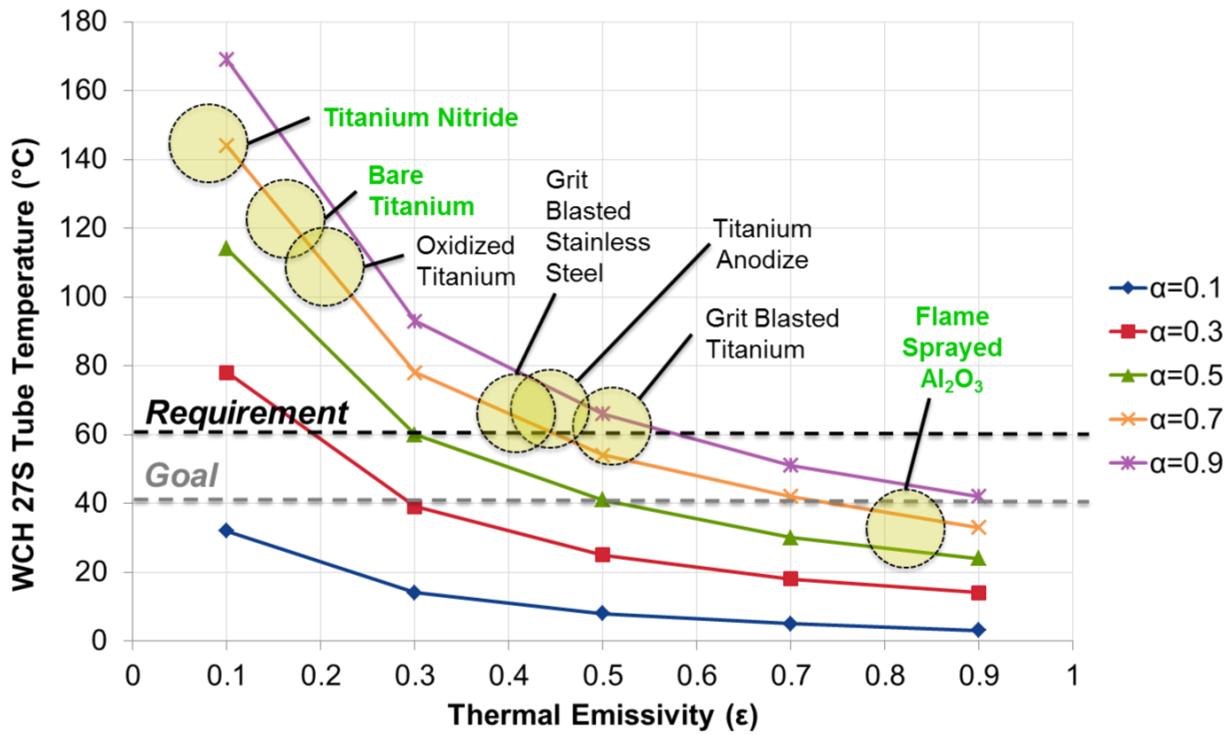

Figure 10: Tube temperature predictions for all combinations of solar absorptivity and thermal emissivity at the WCH 27°S thermal environment. Candidate surface treatments and coatings are overlaid on the chart. Surface treatents and coatings planned for use on the flight design are shown in green bold text.

A number of sensitivity studies also were performed using the detailed models. The remaining sensitivity studies assumed dust covered hot biased grit blasted stainless steel optical properties (ε=0.38, α=0.7). By default, the tubes were assumed to be placed on flat ground, with no ground contact, free convection only, a ground albedo of 0.12 and a ground thermal inertia of 220 $Jm^{-2}K^{-1}s^{-1/2}$ unless noted otherwise. These studies were performed to see if there might be a way to reduce modeling conservatism or use operational constraints so that the tube could meet its thermal requirements. They also provided an indication of how robust the predicted tube temperature is to variations in the assumed tube environment. Even though the flight tubes will not be grit blasted stainless steel, the sensitivity study is beneficial because the same trends should apply to the flight tubes.

The most obvious parameter that affects sample temperature is the landing latitude. However, the Mars 2020 rover is required to be able to land and perform its mission at a landing site within the +/- 30° latitude range. It is not acceptable to constrain the landing latitude in order to make it easier to meet the sample tube temperature requirements. As a result, all of the sensitivity studies performed considers latitudes over the full range. However, sample tube temperature and its effect on science results is being taken into account during the landing site selection process[13].

One parameter that can strongly affect sample temperature is the ground slope on which the sample tube is rests, as well as the orientation of the sample tube relative to the ground slope. Sample temperature sensitivity to ground slope with a downhill pointing sample tube axis is shown in Figure 11, and sample temperature sensitivity to ground slope with a horizontal sample tube axis is shown in Figure 12. The effect of ground slope on tube temperature can be much more pronounced with a downhill pointing sample tube axis than with a horizontal sample tube axis because the tube is angled so that it receives more or less incident sunlight than it would if it was horizontal (similar to the usage for solar cells on Earth). The greatest effect can be seen in equatorial regions since the sun is ~ 65° (90° - 25° inclination of Mars spin axis) above the horizon in the equatorial summer. A 30° ground slope can change the effective elevation angle to as low as 35° or to nearly 90°. However, the effect of ground slope on sample tube temperature is minimal in the WCH 27°S and 30°N environments. In these environments, the sun is already at an elevation angle of ~85 to 88°, so any change in ground slope from flat ground has a small effect.

The effect of ground albedo on sample tube temperature was also explored and is shown in Figure 13. Although an increased ground albedo can decrease ground temperature, which was an effect that was included in the model, it also increases the amount of sunlight that is reflected off the ground and onto the sample tube. The result is that the sample tube temperature can increase by up to 5 °C as a result of increased ground albedo.

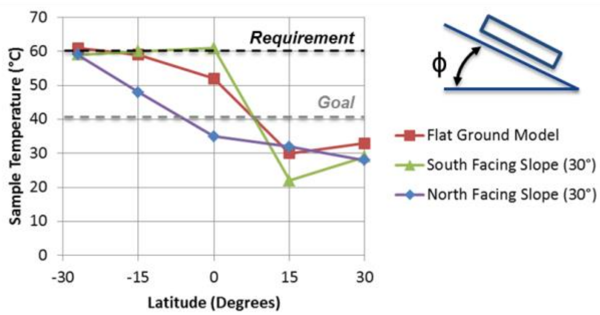

Figure 11: Grit blasted stainless steel sample tube temperature sensitivity to ground slope with a downhill pointing sample tube axis.

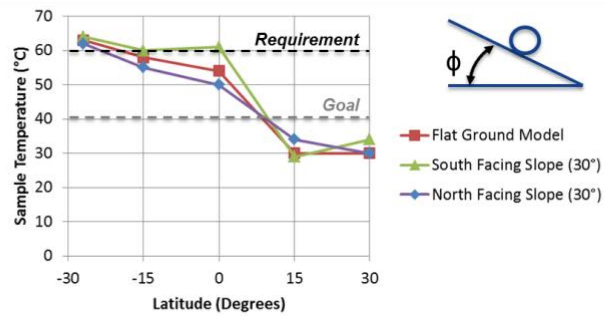

Figure 12: Grit blasted stainless steel sample tube temperature sensitivity to ground slope with a horizontal sample tube axis.

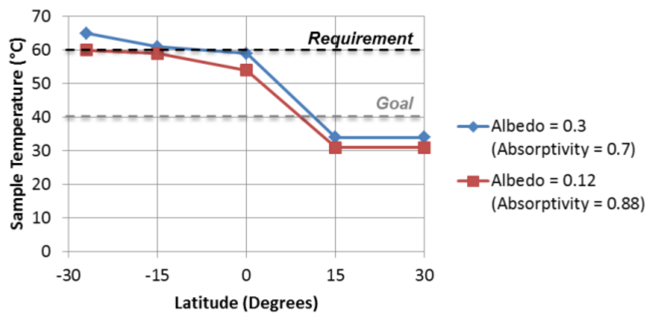

Figure 13: Effect of ground albedo on grit blasted stainless steel sample tube temperature.

One of the most interesting sensitivity studies performed was on the effect of tube-ground contact on sample temperature. This sensitivity study was very interesting, since it is very dependent on the type of regolith found at the tube caching location. This relationship is summarized in Table 3. As the table shows, it is not obvious which type of regolith would be a better place to deposit tubes since both sandy and rocky regolith has advantages and disadvantages. On one hand, sandier regolith would provide better thermal contact between the regolith and tube and would possibly even allow the tube to be “buried” by driving over it, but on the other hand, rockier regolith would have cooler peak ground temperatures and better heat sinking capabilities than sandier regolith. Regardless of ground type, the maximum ground surface temperature is 38 °C, so contact with the ground will always help to cool the sample.

Table 3: Relative effects of regolith type on tube-ground contact

Sandier Regolith (Lower Thermal Inertia)	**Rockier Regolith (Higher Thermal Inertia)**
(+) Better Thermal Contact	(-) Worse Thermal Contact
(+) Easier to “Bury” Tube	(-) Harder to “Bury” Tube
(-) Warmer Peak Ground Temperature	(+) Cooler Peak Ground Temperature
(-) Worse Heat Sink	(+) Better Heat Sink

As a result, an analytical sensitivity study of tube-ground contact was undertaken for both sandy and rocky regolith. For sandier regolith, a thermal inertia of 220 $Jm^{-2}K^{-1}s^{-1/2}$ was assumed, and for rockier regolith a thermal inertia of 350 $Jm^{-2}K^{-1}s^{-1/2}$ was used. Although the range of regolith thermal inertia is greater than this on Mars, thermal inertias much lower than ~ 220 $Jm^{-2}K^{-1}s^{-1/2}$ are often not safe to drive over, and locations with a thermal inertia much greater than ~ 350 $Jm^{-2}K^{-1}s^{-1/2}$ may not occur frequently at all landing latitudes. At both types of ground, four degrees of thermal contact were assumed: perfect contact, G=0.01 W/K, G=0.0045 W/K, and G=0 W/K (no contact). A tube-ground conductance of G=0.01W/K corresponds to roughly 2 mm of gas gap between the tube and ground, and a tube-ground conductance of G=0.0045W/K corresponds to roughly 5 mm of gas gap between the tube and ground. These numbers roughly account for the curved nature of the sample tube, which is why they do not vary by a ratio of 2:5. This level of gas gap is considered reasonable since the tube has complex geometry that could create 2 mm gas gaps between the ground and large parts of the sample tube, even for perfectly flat locations. It should be emphasized that it is impossible to accurately predict the amount of thermal contact between the tube and ground since rocks, pebbles, and uneven regolith could increase or decrease the gas gaps between the tube and ground.

Sample temperature sensitivity to tube-ground contact with ground TI= 220 $Jm^{-2}K^{-1}s^{-1/2}$ and TI= 350 $Jm^{-2}K^{-1}s^{-1/2}$ is shown in Figures 14 and 15, respectively. Tube-ground contact has the potential to provide more cooling when the ground thermal inertia is higher than it does at lower thermal inertia locations. The reason for the distinction is that lower thermal inertia, and hence lower thermal conductivity, regolith is not able to conduct the heat away from the sample tube. Even if a sample tube is half buried in the regolith, the sample tube ends up warming up the regolith that is nearby, diminishing the cooling effects of the ground. A contour plot of a half-buried grit blasted stainless steel tube in this scenario is shown in Figure 16.

Even though the potential for cooling with perfect tube-ground contact is sizeable (10 to 15 °C effect), it is important to remember that the degree of contact is highly uncertain. The effect with realistic levels of tube-ground contact is expected to be < 5 °C at low thermal inertia locations, and < 10 °C at higher thermal inertia locations if a 2 to 5 mm gas gap is relied upon to provide cooling between the tube and ground. As a result, the effects of tube-ground contact are neglected for conservatism in the analysis of the flight tube design.

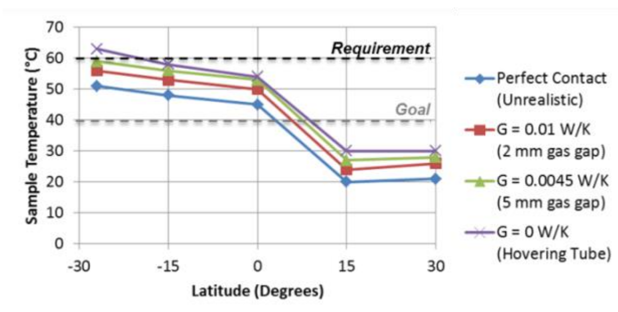

Figure 14: Grit blasted stainless steel sample tube temperature sensitivity to tube-ground contact with ground TI = 220 $Jm^{-2}K^{-1}s^{-1/2}$.

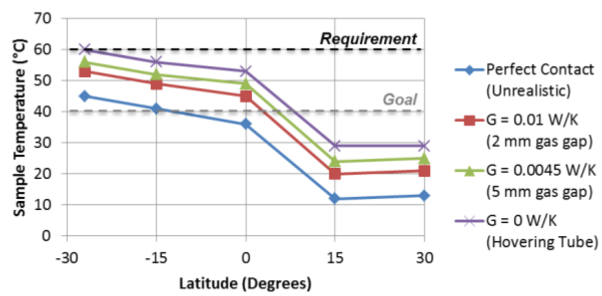

Figure 15: Grit blasted stainless steel sample tube temperature sensitivity to tube-ground contact with ground TI = 350 $Jm^{-2}K^{-1}s^{-1/2}$.

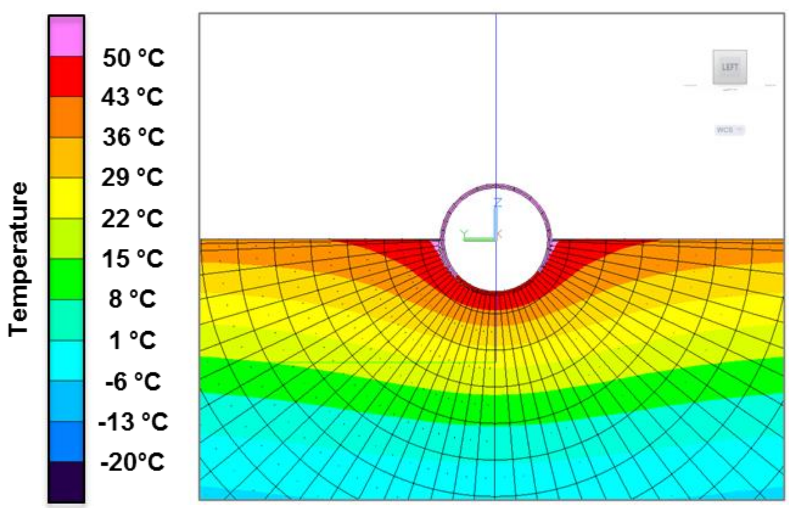

Figure 16: Temperature contour plot of a grit blasted stainless steel tube half-buried in sandy regolith (TI = 220 $Jm^{-2}K^{-1}s^{-1/2}$) in the WCH 27°S environment. The low conductivity regolith is not able to conduct the heat away from the sample and ends up warming up the regolith that is nearby, diminishing the cooling effects of the ground.

VII. Flight Tube Design and Analysis

The primary function of the sample tube is to contain samples, but it also serves a number of other uses. A schematic of the flight sample tube design is shown in Figure 17, and pictures of tubes used in a development test are shown in Figure 18. The tube is constructed of a Ti-6Al-4V body, chosen for its high strength and relatively low density. Flame sprayed Aluminum Oxide (Al_2O_3) is used on much of the tube as a thermal control coating to reduce peak tube temperatures. A bare titanium section is located near the top of the tube for seal robustness, and a thin layer of titanium nitride (TiN) is used on all other non-aluminum oxide coated regions, including the tube interior, to prevent chemisorption of contamination due to its low surface energy.

During drilling, the sample tube is contained within the drill bit. The drill bit and sample tube contact at the bearing race, which is coated with polished Al_2O_3. After drilling is complete, the sample tube is used to transmit torque through the coring system to break off rock cores from the parent rock. The middle section of the tube is eccentric from the bearing race and the back end, which allows a 0.8 mm offset between the rock and the bit centerline when the tube and bit counter-rotate, via a tool that inserts in the back of the tube. This motion creates high shear stress in the rock, causing the rock to break off. The thin-walled section of the tube has been sized to reduce mass and maintain the ability to survive this load. The tube also contains a ball lock mechanism comprised of springs, balls, a plunger, and a retaining ring. The ball lock allows the tube to be locked into a bit during coring operations or in tube storage during launch and traverse on the Martian surface.

In addition to its functions for the Mars 2020 mission, the sample tube also provides features for a potential future sample return mission. The tubes are marked with a unique barcode-like identification that the fetch rover may use to differentiate each sample. Each stripe is created by masking the aluminum oxide, and the pattern corresponds to the binary serialization of each tube, from 1 to 63, as shown in Figure 19. Additionally, there are several indentations around the back end of the tube that are intended to aid tube manipulation and securing for the potential future sample return mission.

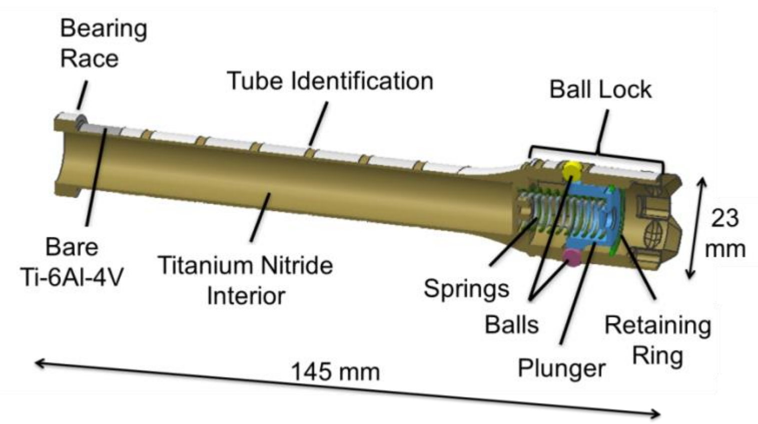

Figure 17: Cross section of empty Ti-6Al-4V flight sample tube design. Components include the bearing race, tube identification, and ball lock mechanism.

Figure 18: Images of tubes used in development tests.

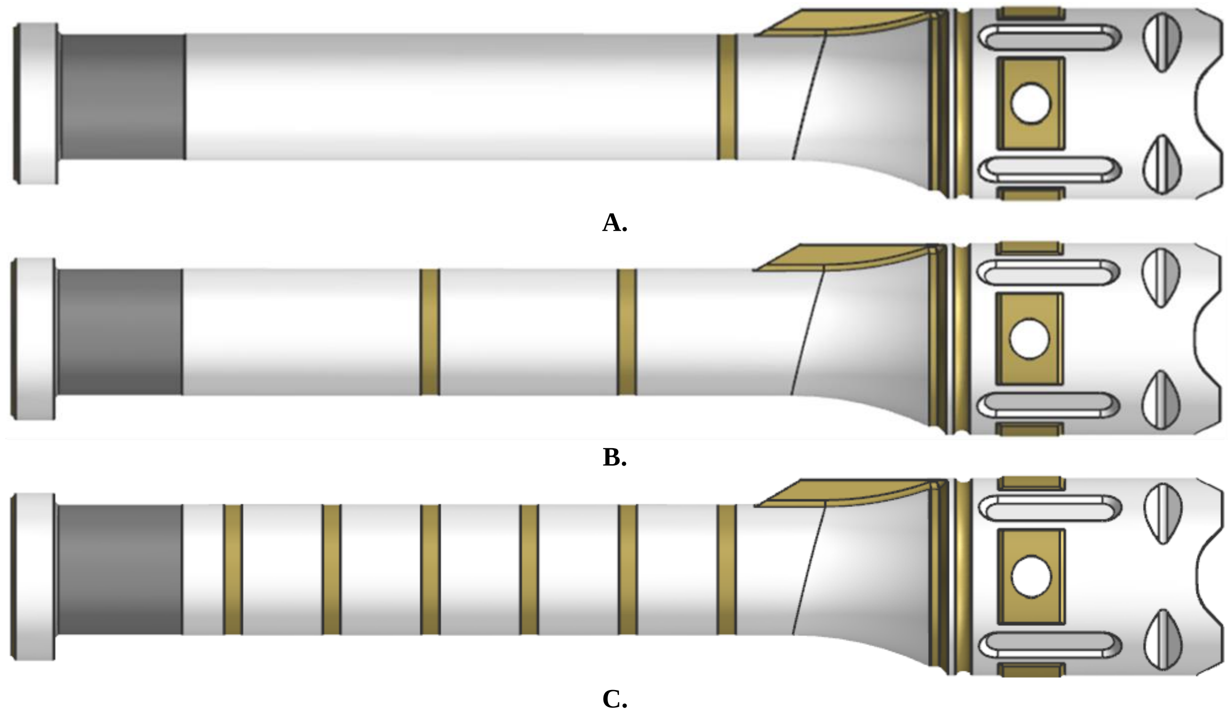

Figure 19: Examples of the sample tube unique identification created via barcode stripes. Images shown correspond to tube binary numbers A) 1 B) 10 and C) 63, which is the worst case hot barcode pattern.

For the worst case hot thermal analysis, the tubes were assumed to be placed on flat ground, with no tube-ground contact, free convection only, a ground albedo of 0.3 and ground thermal inertia of 220 $Jm^{-2}K^{-1}s^{-1/2}$. In addition, the tubes were assumed to have worst case dust coverage, with their solar absorptivity changed to 0.7 for dust, but with thermal emissivity unaffected by the dust accumulation. The worst case hot barcode pattern (Figure 19, C) is used in the thermal analysis, and the thermal emissivity of the tube thermal model is shown in Figure 20. No additional temperature margin was used beyond this set of worst case assumptions.

Worst case hot temperature predictions were made for each of the thermal environments discussed in Section II. Contour plots of peak diurnal tube temperatures are shown in Figure 21, and maximum tube temperature as a function of landing latitude is graphed in Figure 22. The hottest part of the tube (and therefore the sample) occurs in the bare titanium hermetic sealing region near the top of the tube. This corresponds to the uppermost portion of the sample, which may have slightly less science value than the deeper portions since it has been exposed to the Martian surficial environment over geologic time scales. Even with stacked worst case assumptions, the maximum predicted tube temperature is 54 °C, which is below the 60 °C temperature requirement. In addition, the maximum predicted tube temperature is below the 40 °C goal at 2 of the top 3 potential landing sites.

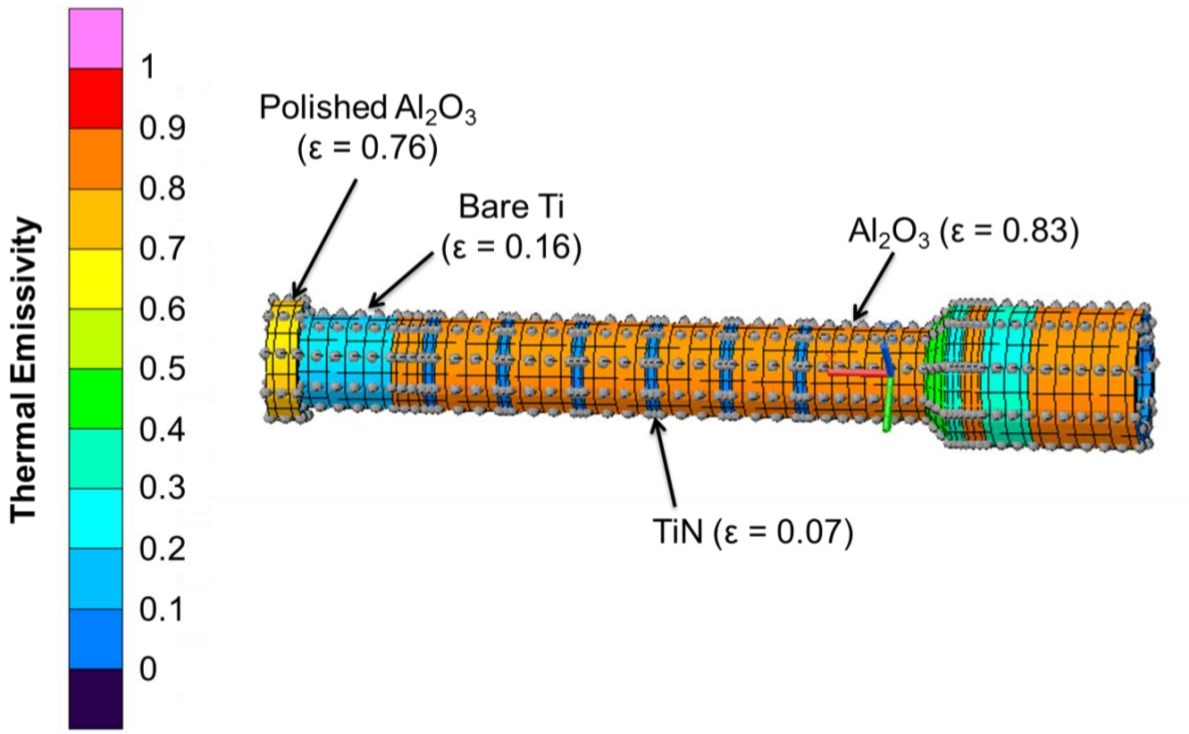

Figure 20: Thermal emissivity contour plot of the tube thermal model.

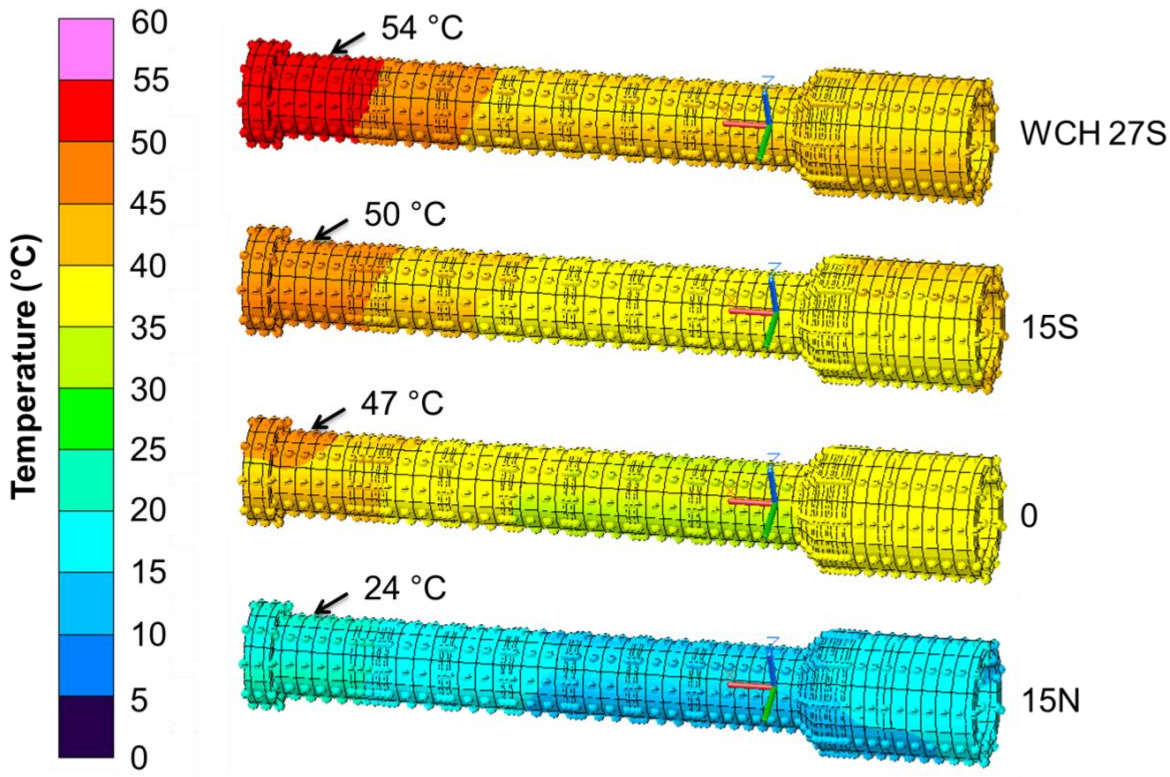

Figure 21: Contour plots of peak diurnal tube temperatures in selected thermal environments.

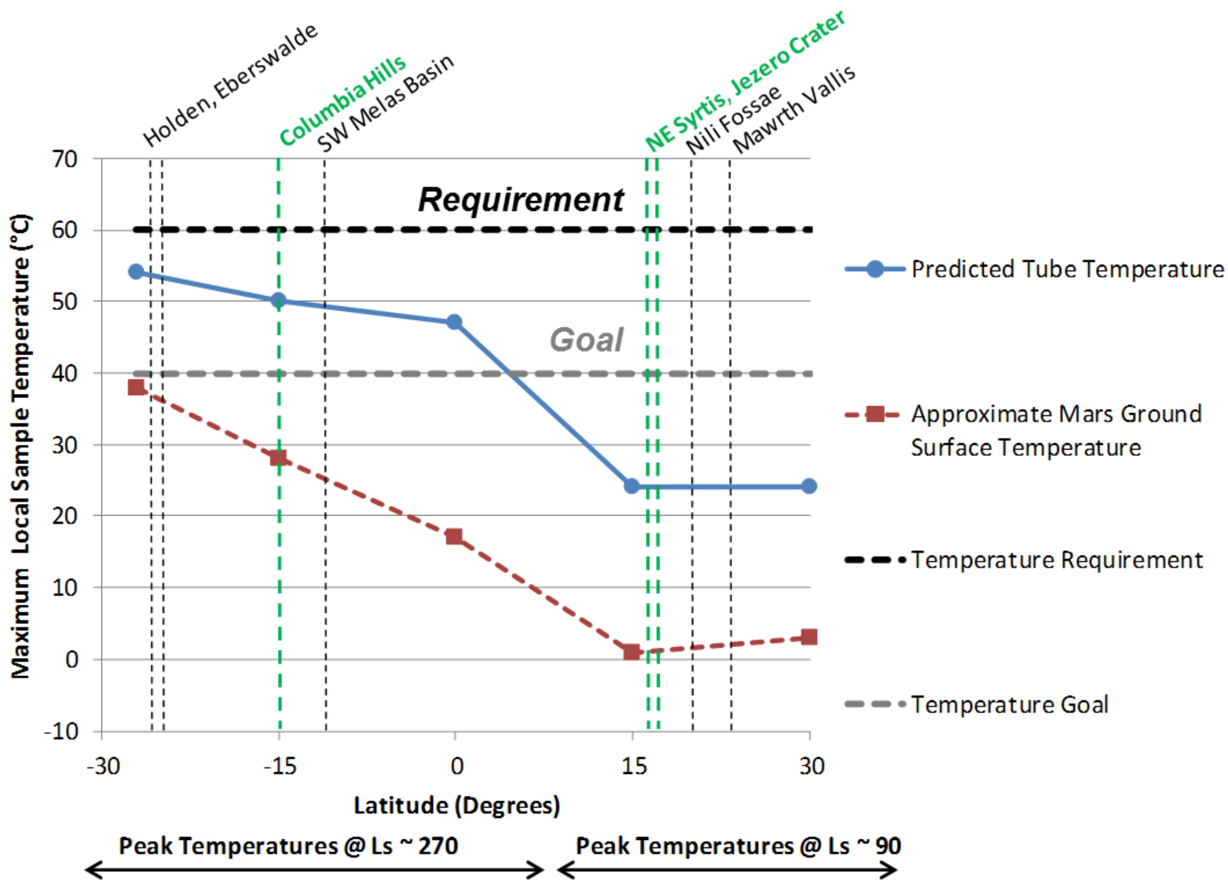

Figure 22: Maximum sample tube temperature for the five different thermal environments. The top 8 landing sites are represented by vertical dashed lines, with the top 3 landing sites highlighted in green. Temperatures are for flat ground locations, roughly corresponding to the hottest part of the year at each latitude.

VIII. Operational Considerations

Although the Mars 2020 mission is still several years away, the mission operations strategy is already being planned[17]. When collected samples are cached, they can be placed at a desirable caching location according to the mission needs and desires. Potential future return missions should be able to identify the caching location to within ~1 m using orbital imagery and to within ~1 cm using rover cameras[17]. It is also likely that the mission operations team will not want to deposit tubes near geologic features such as sand dunes that can migrate over time, or on the side of a hill where tubes could roll and be difficult to find again in the future.

From a thermal standpoint, once tubes are cached on the Martian surface, it is important for the rover to avoid driving over top of the tubes. The rover is powered by a Radioisotope Thermoelectric Generator (RTG) which can significantly warm the ground underneath the rear end of the rover[11]. Driving over the tubes poses a risk that a mobility fault could subject the tubes to an extended period of exposure to temperatures significantly warmer than shown in this analysis. In addition, there may be a desire to place tubes at a location which will reduce maximum tube temperatures, especially if one of the warmer southern landing sites is selected. Of course, if peak predicted sample temperatures are below room temperature (~25 °C), then this is completely unnecessary because the collected samples will surely be exposed to room temperature on a possible future return to Earth. One possible way to reduce tube temperature using operational constraints is to look for very high thermal inertia regions where peak local ground and atmospheric temperatures are reduced[11]. This effect has also been observed in the flight data from the MSL Curiosity rover at Yellowknife bay[18]. This strategy might be worth exploring in more detail in the future, depending on mission needs and desires.

IX. Conclusion and Future Work

The sample tube design for the Mars 2020 mission recently completed its detailed design review (DDR). Only minor changes, if any, are expected between now and launch of the Mars 2020 spacecraft. A significant effort has gone into coming up with a sample tube thermal design which allows the tube and collected sample to remain below the maximum allowable temperature of 60 °C at any landing site in the +/- 30° latitude range. The maximum predicted sample temperature at the warmest possible Mars 2020 landing site with worst case assumptions is 54 °C. In addition, tube temperatures might remain below the 40 °C goal depending on which landing site is selected.

Tube temperatures are very sensitive to the tube surface treatments and coatings, which is why flame sprayed Aluminum Oxide (Al_2O_3) is used extensively on the tube as a thermal control coating. Bare titanium is used in the hermetic seal region for sealing robustness, and titanium nitriding is used extensively in other regions for its ability to control tube contamination. Tube temperature is also strongly affected by dust deposition, which cannot realistically be controlled over a 10 year surface mission. Local ground albedo, ground slope, tube-ground contact, and ground thermal inertia can also affect maximum sample tube temperature to a moderate degree.

As the Mars 2020 mission nears launch, it may be useful to perform additional tube temperature predictions using the thermal environment of the selected landing site as opposed to the approximate environments that were used in this work. In addition, more work may be useful for informing the mission operations team on the best place to cache sample tubes to minimize their temperature.

Acknowledgments

This research was carried out at the Jet Propulsion Laboratory, California Institute of Technology, under a contract with the National Aeronautics and Space Administration. The authors wish to thank Mark Hetzel for his assistance with optical property measurements. Reference herein to any specific commercial product, process, or service by trade name, trademark, manufacturer, or otherwise, does not constitute or imply its endorsement by the United States Government or the Jet Propulsion Laboratory, California Institute of Technology.

References

[1]Farley, K., "Mars 2020 Project Update," Committee on Astrobiology and Planetary Science, September 17, 2015. Accessed from http://sites.nationalacademies.org/cs/groups/ssbsite/documents/webpage/ssb_169425.pdf on 12/9/2016.

[2]"Mars 2020 Rover Depot Caching Strategy," Accessed from http://mars.nasa.gov/mars2020/mission/timeline/surface-operations/ on 12/9/2016.

[3]Witze, A., "The $2.4-billion plan to steal a rock from Mars," *Nature*, vol. 541, pp. 274–278, 19 January 2017.

[4]Farley, K.A., and Williford, K.H., "Seeking signs of life, and more: NASA's Mars 2020 mission," *EOS: Earth & Space Science News*, vol. 98, no. 1, 11 January 2017.

[5]Redmond, M., Berisford, D., and Novak, K., "Water and Helium Leak Rate Requirements for a Mars Sample Sealing System," *45th International Conference on Environmental Systems*, Bellevue, WA, July 12-16, 2015.

[6]Bhandari, P., Redmond, M., and Kempenaar, J., "Mars Sample Thermal Control During Mars Ascent and Orbit," *46th International Conference on Environmental Systems*, Vienna, Australia, July 10-14, 2016.

[7]Perino, S., et al., "The Evolution of an Orbiting Sample Container for Potential Mars Sample Return," *IEEE Aerospace Conference*, Big Sky, MT, March 4-11, 2017.

[8]Beaty, D.W., et al., "Recommended Maximum Temperature for Mars Returned Samples," *47th Lunar and Planetary Science Conference*, The Woodlands, TX, March 21-25, 2016.

[9]Novak, K., Kempenaar, J., Redmond, M., and Bhandari, P., "Preliminary Surface Thermal Design of the Mars 2020 Rover." *45th International Conference on Environmental Systems*, Bellevue, WA, July 12-16, 2015.

[10]Farias, E., Redmond, M., Karp, A., Mechentel, F., Story, G., and Shotwell, R., "Thermal Cycling for Development of Hybrid Fuel for a Notional Mars Ascent Vehicle," *AIAA Propulsion and Energy Forum*, Salt Lake City, UT, July 25-27, 2016.

[11]Farias, E., Redmond, M., Bhandari, P., Kempenaar, J., and Novak, K., "Thermal Modeling of Mars Ground for Surface Missions," *47th International Conference on Environmental Systems*, Charleston, SC, July 16-20, 2017.

[12]Golombek, M.P., et al., "Downselection of Landing Sites Proposed for the Mars 2020 Rover Mission," *47th Lunar and Planetary Science Conference*, The Woodlands, TX, March 21-25, 2016.

[13]Witze, A., "Three sites where NASA might retrieve its first Mars rock," *Nature*, vol. 542, pp. 279–280, 11 February 2017.

[14]Gilmore, G. (ed.), "Spacecraft Thermal Control Handbook," 2nd ed., The Aerospace Corporation, 2002.

[15]Redmond, M., and Mastropietro, A.J., "Thermophysical and Optical Properties of Materials Considered for use on the LDSD Test Vehicle," *45th International Conference on Environmental Systems*, Bellevue, WA, July 12-16, 2015.

[16]Landis, G.A., et al., "Dust and Sand Depositon on the MER Solar Arrays as Viewed by the Microscopic Imager," *37th Lunar and Planetary Science Conference*, League City, TX, 2006.

[17]Farley, K.A., and Williford, K.H., "Scientific Rationale for Depot Caching on Mars 2020," Retrieved from marsnext.jpl.nasa.gov/documents/Mars_2020_Caching-Strategy_V4.pdf on 2/17/2017.

[18]Cucullu, G.C., Zayas, D., Novak, K., and Wu, P., "A Curious Year on Mars – Long Term Thermal Trends for Mars Science Laboratory Rover's First Martian Year," *44th International Conference on Environmental Systems*, Tuscon, AZ, July 13-17, 2014.